Chapter 4

Experimental Investigation of Load-Sharing in Piled-Rafts

4.1 Introduction

The expense of large field tests makes it challenging to conduct several trials in a brief amount of time. For this reason, laboratory tests have traditionally been prevalent. Further, monitoring and achieving desired soil characteristics is easier under controlled laboratory circumstances. With a proper understanding of the model's behaviour, it can be more feasible to apply it in the field reliably and cost-effectively.

The objectives of the current study focus on exploring the load-settlement behaviour of piled rafts with various configurations. The following sections provide details on test materials, model configurations, and testing techniques that have been used. Multiple test trials were conducted on both sand and clay to attain the study's objectives. To verify the outcomes, the tests were repeated twice wherever required. The box dimensions used for the tests were chosen so that the boundaries wouldn't impact the test results. Hence, it was decided to use a soil bin with a depth at least twice the longest pile length (Sinha and Hanna, 2016). Also, the bin width was assumed to be five times the raft width.

4.2 Testing materials and equipment

4.2.1 Test soils

Locally available Son River sand and clay from the Ganga basin were used in the current investigation. The sand and clay are exclusive selected in the study due to their representativeness in geotechnical engineering practice and their distinct granular and cohesive behaviours, capturing a broad spectrum of real-world geotechnical conditions. This simplification enhances analysis manageability and practicality while allowing engineers to develop insights into fundamental soil-structure interaction mechanisms applicable across various soil types. The Son River is one of the largest tributaries of the Ganges, and its sand is widely used in construction across India. The sand particles are yellowish-brown and coarser in size. The used sand and clay were collected from the nearest construction site. Undesirable materials such as roots, plastics or organic wastes were physically removed from the soils and were completely dried. Figure 4.1 displays the clay and sand samples that were used.

(a) Sand (b) Clay

Figure 4.1: Materials used in the test

The Index properties of soils used in engineering establish their classification and identification. Table 4.1 lists some of the key index properties of the sand and clay utilised in the current research. Figure 4.2 shows the particle size distribution curves of the used sand. Such a curve represents the distribution of the soil sample into different fractions depending on their sizes. Figure 4.3 graphically illustrates

the relationship between the density index and the voids ratio for the sand. The coefficient of uniformity (C_u) and coefficient of curvature (C_c) were obtained as 2.71 and 0.91, respectively.

Consequently, the sand sample can be categorized as poorly graded sand (SP) as per IS: 1498 (1970) (Reaffirmed, 2021). Furthermore, shear parameters of sand were computed using direct shear tests and triaxial tests as per IS: 2720 (Part 13) (1986) and IS: 2720 (Part 11) (1993), respectively. The friction angle was found to be approximately 39°. Specific gravity was obtained to be 2.67 using the Pycnometer method. The minimum and maximum dry unit weights of the sand sample were determined as per IS: 2720 (Part 14) (1983) as 1.52 and 1.73, respectively. Finally, the relative density of the sand was determined to be 65%, indicating that it is dense sand.

Table 4.1: Physical properties of sand and clay

Parameters	**Sand**	**Clay**
Specific Gravity	2.67	2.58
Minimum dry unit weight (kN/m^3)	14.90	-
Maximum dry unit weight (kN/m^3)	16.96	-
$D_{10}(mm)$	0.35	0.004
$D_{30}(mm)$	0.55	0.015
$D_{60}(mm)$	0.95	0.075
Uniformity Coefficient (C_u)	2.71	18.75
Coefficient of Curvature (C_c)	0.91	0.75
Liquid Limit	-	40.50%
Plastic Limit	-	22.68%
Soil Type	SP	CI

In the case of clay, sieve analysis and hydrometer analysis were performed in accordance with IS 2720 (Part 4)-1985. The corresponding curves are illustrated in Figure 4.4 and Figure 4.5. The liquid limit and plastic limit tests were performed using procedures mentioned in IS 2720 (Part 4)-1985 [43], which were found to be 40.50% and 22.68%. Finally, according to IS1498-1970 [42], the Casagrande plasticity chart identified the used clay as clay with intermediate plasticity (CI).

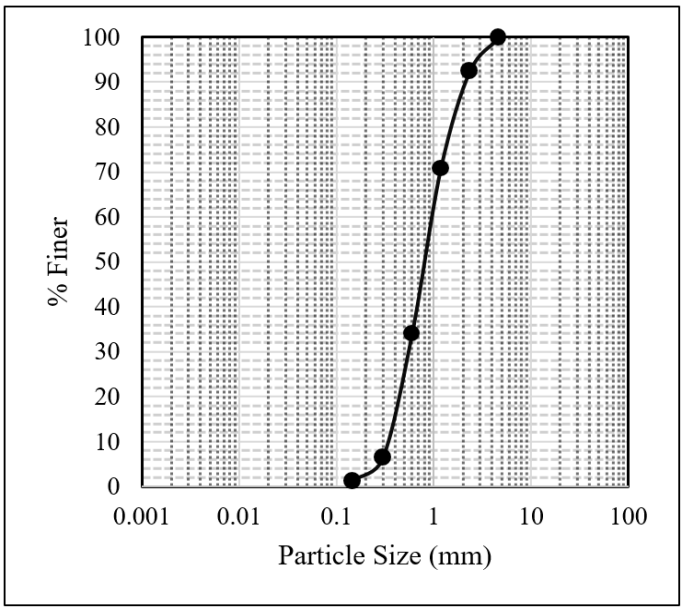

Figure 4.2: Particle Size Distribution of Sand

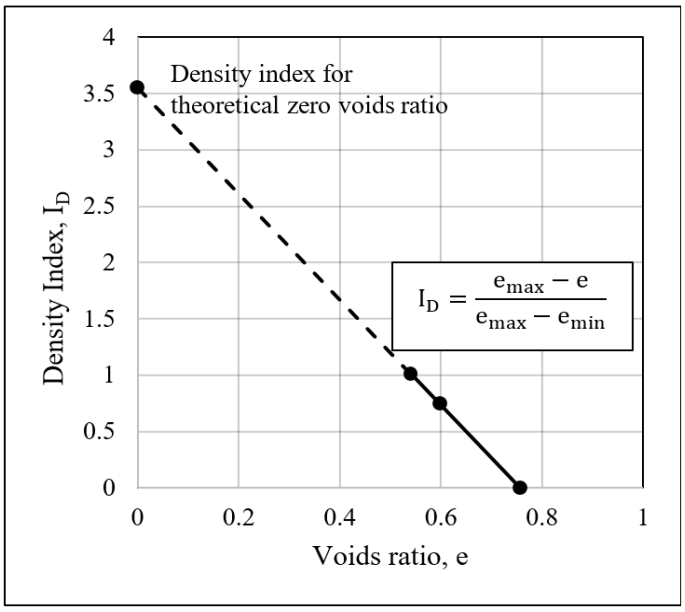

Figure 4.3: Density Index v/s Voids Ratio

4.2.2 Raft and Piles

A square steel plate with sides of $150mm$ and a thickness of $10mm$ was used to model the raft. To fasten the model piles in prescribed layouts, 9 holes with $50mm$ spacings were made. Depending on the required configurations, the piles were fastened to these holes and tightened using the nuts. The bolts were used to plug holes in the raft. Figure 4.6 depicts a model piled-raft with 9 piles attached

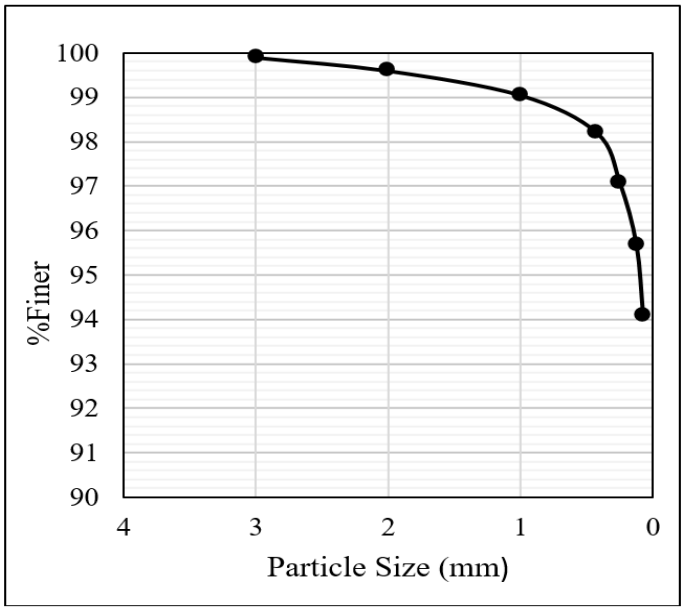

Figure 4.4: Sieve Analysis

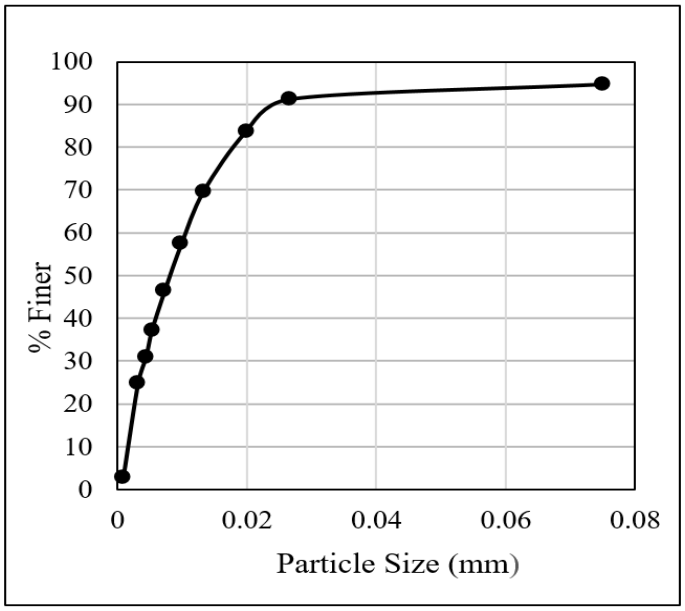

Figure 4.5: Hydrometer Analysis

in a proper arrangement. The current investigation used 1, 4, 5 and 9 piles with lengths of $160mm, 260mm$ and $360mm$. The cross-sections of all 27 model piles were circular, with a diameter of $12mm$. Mechanical properties of the model steel piles are presented in Table 4.2. Elastic modulus and Poisson's ratio of the piles were found to be $200GPa$ and 0.28, respectively.

These piles were threaded on the upper side and attached to the raft using nuts. To achieve total fixity, the bolts were provided on both sides of the raft and tightened

Table 4.2: Mechanical properties of steel piles

Parameters	**Values**
Unit Weight (kN/m^3)	72.43
Minimum yield strength	355.53
Maximum ultimate strength	511.62
Minimum % elongation	23.33

with a wrench. The different configurations of model piled-rafts used in the study are shown in Figure 4.7.

Figure 4.6: Model piled-raft

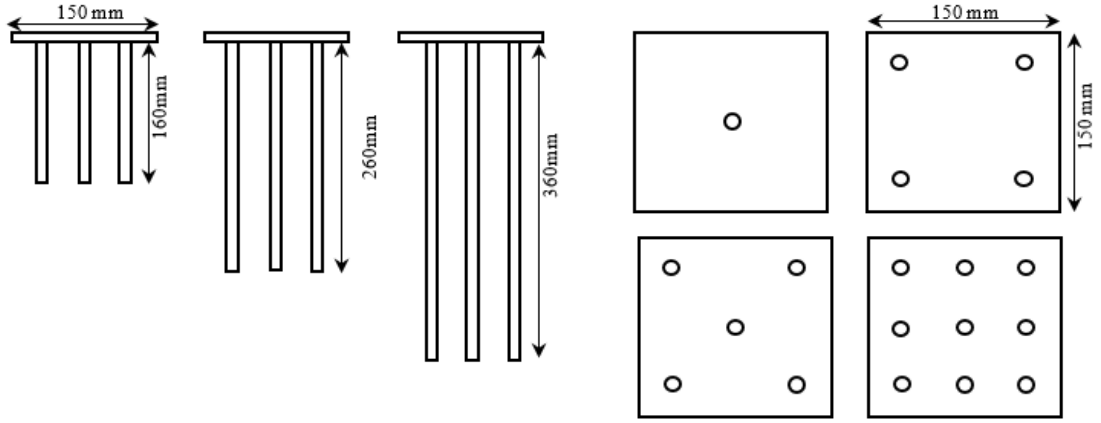

Figure 4.7: Different configurations of model piled-raft

Relative stiffness factor (K_{rc})

Based on the relative stiffness factor (K_{rc}) between soil and piles, Poulos and Davis (1980) categorised piles into two types: rigid and flexible. Mathematically, the relative stiffness factor K_{rc} is defined as follows:

$$K_{rc} = \frac{E_p I_p}{E_s L^4} \tag{4.1}$$

Here, E_p represents the elastic modulus of the model pile, and E_s denotes the secant modulus of the supporting soil. L denotes the embedded length of the pile, and I_p represents the moment of inertia of the model pile. A pile is considered rigid if K_{rc} is greater than (10^{-2}) and while it is classified as flexible if K_{rc} is less than (10^{-2}). With L/D ratios of 13.33, 21.67, and 30, the piles considered for the present study fall into the category of flexible piles.

Scaling Law

The dimensions and proportions of the model need to be adjusted to represent the prototype accurately. To achieve this, scaling is performed using specific scaling laws. Various researchers have suggested scaling laws to imitate the prototype using an equivalent experimental model. Both laboratory and prototype models exhibit direct proportionality in dimensions such as length and width. However, parameters like moment of inertia and flexural rigidity cannot be directly scaled proportionally. Hence, distinct scaling laws are utilized to accommodate these variations. Table 4.3 presents some of the parameters along with the scaling factors. The present study applies the scaling law proposed by Alnuaim et al. (2017), which can be represented as:

$$(EI)_p = n^{3.64}(EI)_m \tag{4.2}$$

Here, EI represents the flexural rigidity of the pile, while p and m denote the

prototype and model, respectively. The symbol $'n'$ represents the scaling factor and is commonly used to represent the ratio of a characteristic dimension of a model to the corresponding dimension of a prototype. It is important to note that the primary objective of this paper is not to replicate a specific prototype. Instead, it aims to investigate and analyse the behaviour of piled rafts within layers of sand and clay. Moreover, the existing literature on experimental analysis has utilized steel raft dimensions of $150mm \times 150mm$ (Elwakil and Azzam, 2016) and $300mm \times 300mm$ (Kumar and Kumar, 2018). Therefore, it is reasonable to justify the adoption of a square steel raft with dimensions of $150mm \times 150mm$ in the current paper.

Table 4.3: Scaling factors used in the present study

Parameters	**Scaling law**
Pile length	$1/n$
Pile diameter	$1/n$
Raft thickness	$1/n$
Density	1
Flexural rigidity	$(EI)_p/n^{3.64}$
Stress	$1/n$
Strain	1

4.2.3 Soil Bin

The entire experimental work was carried out in a soil bin with dimensions of $750mm \times 750mm \times 800mm$. Wooden plies were used to construct the bin, and an iron framework was used to stiffen the bin. The framework comprised multiple iron rods that were welded together and wrapped around the wooden bin to prevent the connections from opening. The dimensions of the bin were chosen to ensure that the influence zone of the foundation remained within the boundaries.

4.2.4 Loading Mechanism

A manually operated hydraulic jack was used to load the foundation model. The mechanism of the hydraulic jack is designed to pull self-lubricating fluid from its reservoir and release it into a cylinder that further applies the loads. This

incompressible fluid helps create pressure between the reservoir and the cylinder through a pump plunger. The plunger draws the fluid from the reservoir on each stroke via a suction valve. The fluid is released into the cylinder after being pushed via a check valve. The suction valve closes after the fluid has passed through the check valve, creating oil pressure inside the cylinder. This oil pressure pushes the cylinder to exert loads.

A proving ring with a maximum capacity of $15kN$ was mounted at the centre of the raft to measure the amount of load applied. Two dial gauges of accuracy $0.01mm$ were attached to the raft to determine its vertical settlement.

Dial gauge comprised of a gauge for assessing the displacement that the needle has gone through during the entire process. The gauge was fixed to steel rods to adjust the position and height of the needle. Needles of dial gauges were placed at the extreme corners of the raft, and the gauge was clamped using a magnetic base.

4.3 Test procedures

The following sections cover all of the test procedures for the current experimental investigation. The unpiled raft was investigated first, then the piled raft, and finally, the group piles. Figures 4.8 and 4.9 illustrate the schematic diagram and the actual experimental arrangement.

4.3.1 Preparation of soil bed

Soil bed preparation is crucial in conducting experimental analyses of small-scale model piled rafts. It involves meticulous planning and execution to represent real-world soil conditions accurately. The soil is carefully selected based on its gradation and properties, such as particle size, shape, and angularity, to resemble the target soil profile closely. The soil is then evenly spread and compacted layer by layer, ensuring uniform density throughout the bed. The behaviour of small-scale model piled rafts under various loading situations can be thus precisely modelled in an

experimental setup by carefully preparing the soil bed.

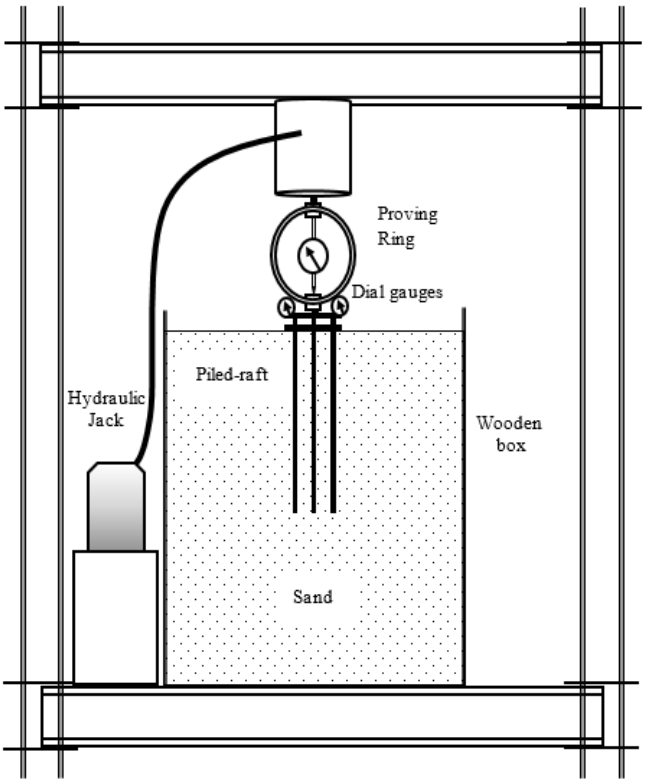

Figure 4.8: Schematic diagram of the experimental arrangement

Figure 4.9: Actual experimental arrangement

The soil bed was prepared using the dry pluviation method, where the soil was allowed to fall freely from a predetermined height at a consistent rate. By employing a pluviation height of 750mm, a relative density of 70% was achieved. Regular intervals were marked within the container to create the sand bed, and a measured amount of sand was added to each marking to maintain the desired density. A $4.9kgs$ circular plate with a diameter of $150mm$ and a thickness of $25mm$ was used to compact the sand. This activity was repeated until the bin's full height of $750mm$ was reached. The top $50mm$ of the soil bin was left empty to prevent any overflow during loading. The respective densities were maintained throughout the soil bin with a tolerance of 0.5%. The topmost layer of the soil surface was properly levelled and verified using a spirit level to ensure the proper placement of the raft. The aforementioned process was repeated for each set of tests.

The clay bed preparation followed a procedure similar to that described by Rao et al. (1998). The clay was combined with the appropriate amount of water in a separate mixing tank until it reached a consistency (I_c) of 0.30, representing the clay used in the study. The clay was compacted in layers using the same procedure previously described for sand. Measurements of the water content, density, and undrained shear strengths at different depths within the soil bed were taken to confirm homogeneity.

4.3.2 Driving of piled-raft

The model foundation was positioned at the centre and slowly inserted into the soil using the hydraulic jack. In the case of piled rafts, the process was continued until the raft's bottom came into contact with the soil and thus completely supported over it. Likewise, the raft was kept 30mm above the surface in the case of group piles.

4.3.3 Taking observations

The jack was lowered until it came in contact with the proving ring, and dial gauges started responding. Further, the readings in all the dial gauges were corrected to

zero. Centring of the raft was done using a plumb bob suspended through the centre of the jack to ensure no eccentricity. Concentric vertical loading was hence employed through the jack in increments. The load was continued till the full extension of the jack length. Since the loading was concentric and rotation of the raft was not allowed, the dial gauge readings were nearly identical. The load readings were observed at every 5 divisions of the proving ring, having a calibration factor of 1.18. Corresponding raft settlements in dial gauges were noted down. These dial gauge readings were averaged to acquire the average settlement. Ultimately, the load versus settlement curves were potted for each model configuration.

4.4 Results and discussions

The following sub-sections discuss the behaviour of piled rafts with different configurations. The variation in pile lengths and pile numbers is analysed and plotted in the current experimental investigations as load-settlement curves.

El-Garhy et al. (2013) used $10mm$ and $25mm$ as the index parameters for the experimental study. The ultimate load capacity was adopted by Bowles (1997) as the load at $60mm$ of settlement. However, the load-settlement curves in the present study do not show a considerable change at the initial settlement phases, and the change may be better noticed in the later stages. Besides, the observations are restricted to $50mm$ settlement of raft due to the limitation of dial gauges. As a result, a higher raft settlement of $40mm$ has been chosen as the index parameter in the current research.

4.4.1 Effect of number of piles (n_p)

The model raft was initially rested on the foundation soil, and its behaviour was assessed. It was important to examine the raft's behaviour to compare it with the behaviour of model piled-rafts. The number of piles varied from 1 to 9 to analyse the effectiveness of attached piles.

Figures 4.10 and 4.11 indicate that as the number of piles increases, the load-bearing capacity of the piled raft also increases. An unpiled-raft in the host sand was observed to have a load-bearing capacity of $3.6kN$ at $40mm$ settlement. This capacity increased to $4.5kN, 8kN, 10kN$, and $14kN$, when the number of piles affixed to the raft varied, measuring 1, 4, 5, and 9, respectively. Similarly, the load capacity improved from $3.6kN$ to $5.2kN, 7.9kN, 8.8kN$ and $10.2kN$, in the case of clay. The results are anticipated as the additional piles interact with the underlying soil over a wider surface area. Consequently, the piles can resist a greater amount of the load. It can be confirmed by the literature reported (Kumar and Kumar, 2018).

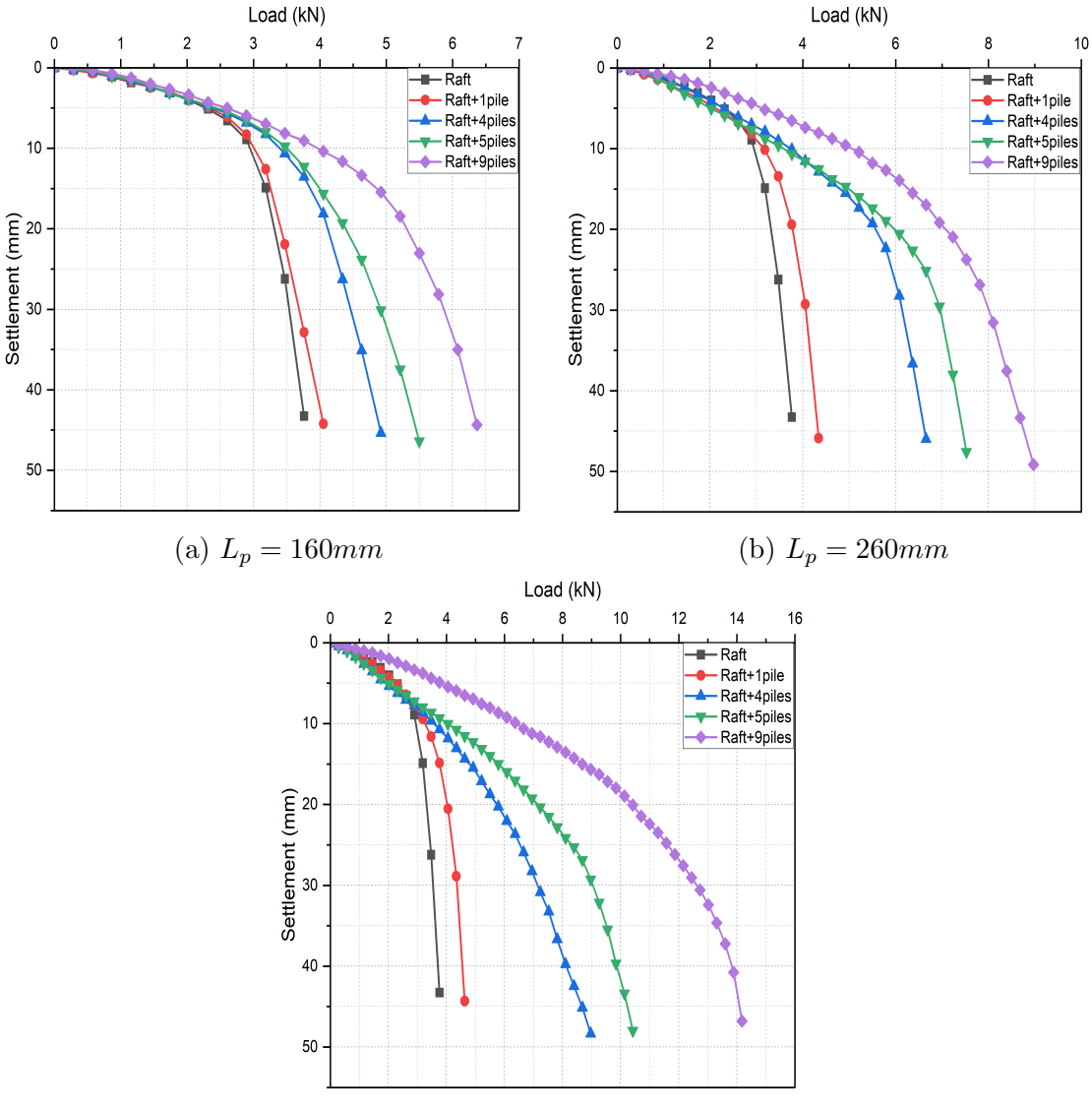

(a) $L_p = 160mm$ (b) $L_p = 260mm$

(c) $L_p = 360mm$

Figure 4.10: Effect of number of piles on piled raft behavior in sand

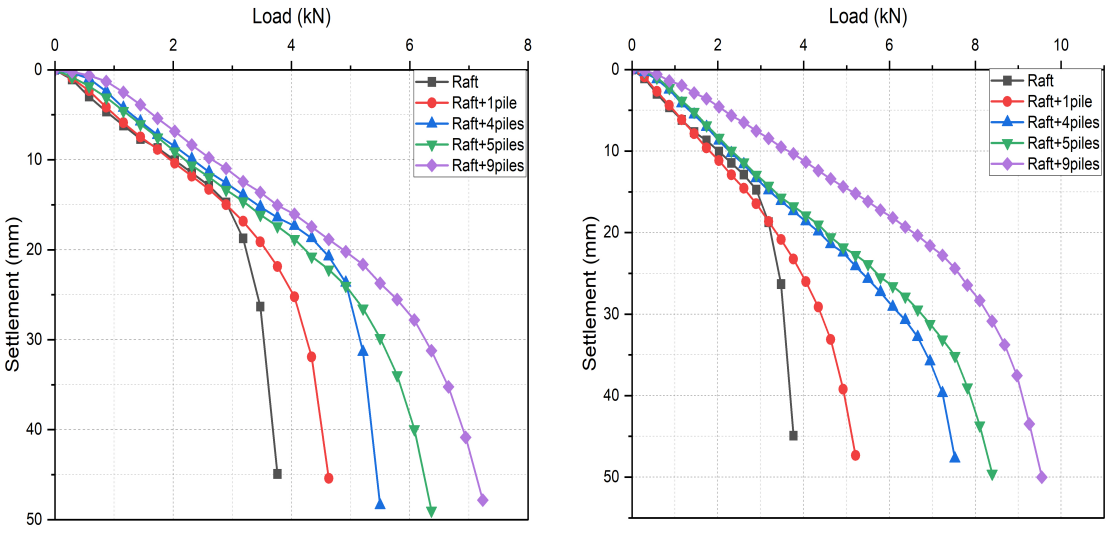

(a) $L_p = 160mm$ (b) $L_p = 260mm$

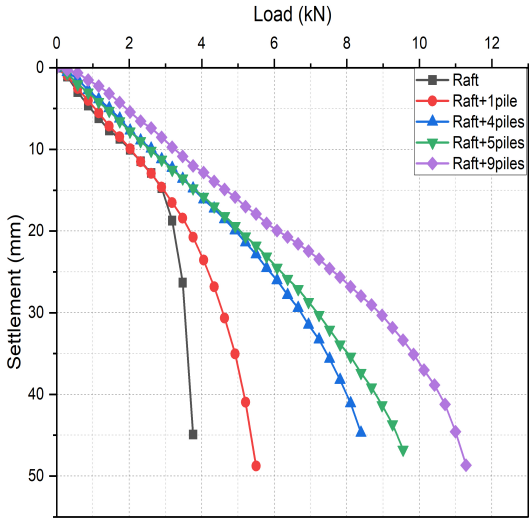

(c) $L_p = 360mm$

Figure 4.11: Effect of number of piles on piled raft behavior in clay

However, Poulos (2008) noted that adding more number of piles to improve the performance of a piled-raft foundation may not always be advantageous. This is because once a certain threshold is crossed, very little benefit is observed, which could result in an uneconomical decision.

4.4.2 Effect of pile length (L_p)

The impact of varying pile lengths has been presented using load-settlement curves in Figures 4.12 and 4.13. As the length of the piles affixed to the raft varied, measuring $160mm, 260mm$, and $360mm$, the load capacity in the case of sand further improved

to $6.2kN, 8.5kN$, and $13.8kN$, respectively at 40mm settlement. Although this load capacity is for a piled raft with 9 piles, similar increases can be noticed for different numbers of piles as well. It can also be observed that piled rafts over sand and clay with any number of piles exhibit a similar trend, and the load capacity in the clay case is also enhanced by almost $92\%, 150\%$, and 192%, respectively.

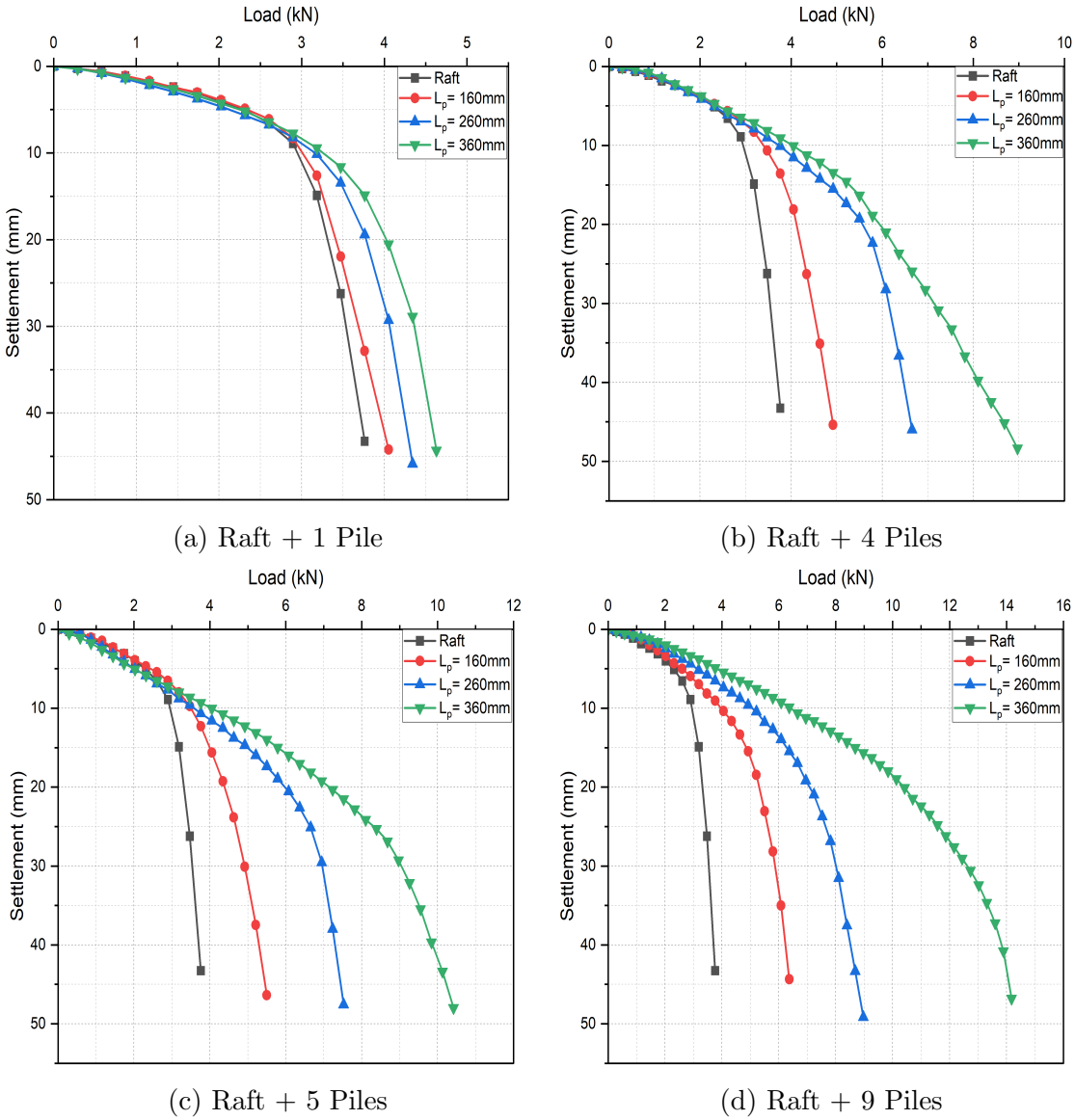

(a) Raft + 1 Pile

(b) Raft + 4 Piles

(c) Raft + 5 Piles

(d) Raft + 9 Piles

Figure 4.12: Effect of pile length on piled raft behavior in sand

It is evident that when pile lengths increase, surface area also increases. It suggests an improvement in shear strength and, eventually, an increase in the load capacity. This supports the findings that have been documented in the literature (Elwakil and Azzam, 2016) reporting that piled rafts with longer piles sustain greater loads.

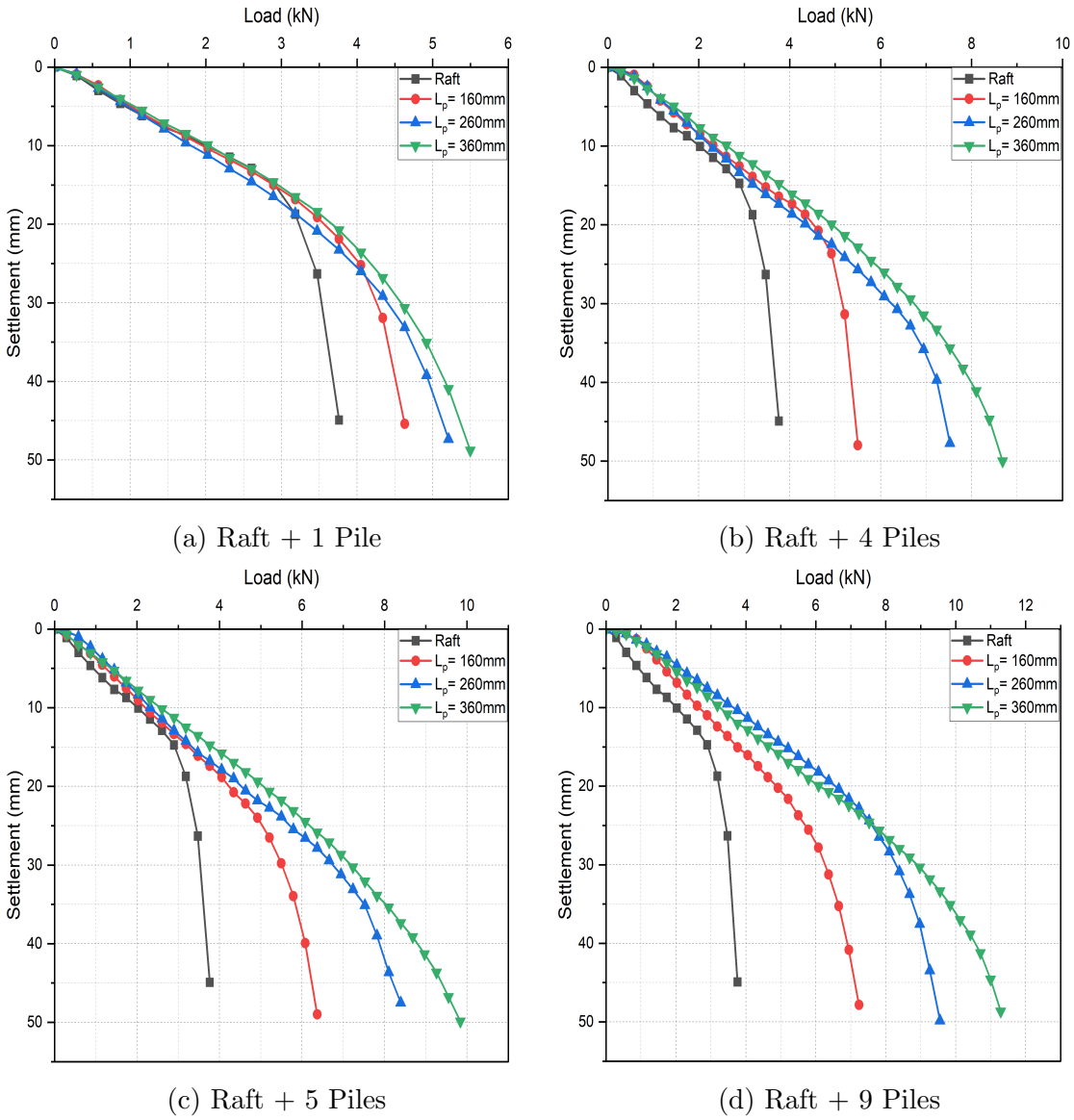

(a) Raft + 1 Pile

(b) Raft + 4 Piles

(c) Raft + 5 Piles

(d) Raft + 9 Piles

Figure 4.13: Effect of pile length on piled raft behavior in clay

4.4.3 Effect of pile numbers in pile groups

The behaviour of pile groups was first studied to compute the load sharing in piled rafts. Figure 4.14 illustrates the comparison of model pile foundations with different numbers of piles. The pile length of $360mm$ was only considered. The pile foundation model was inserted into the soil such that the raft serving as the pile cap was not in contact with the soil surface and raised $30mm$ above it.

Using $25mm$ as the reference settlement level in the pile group over sand and clay, the single pile carried a load of $0.25kN$ and $0.75kN$, respectively. It was found that

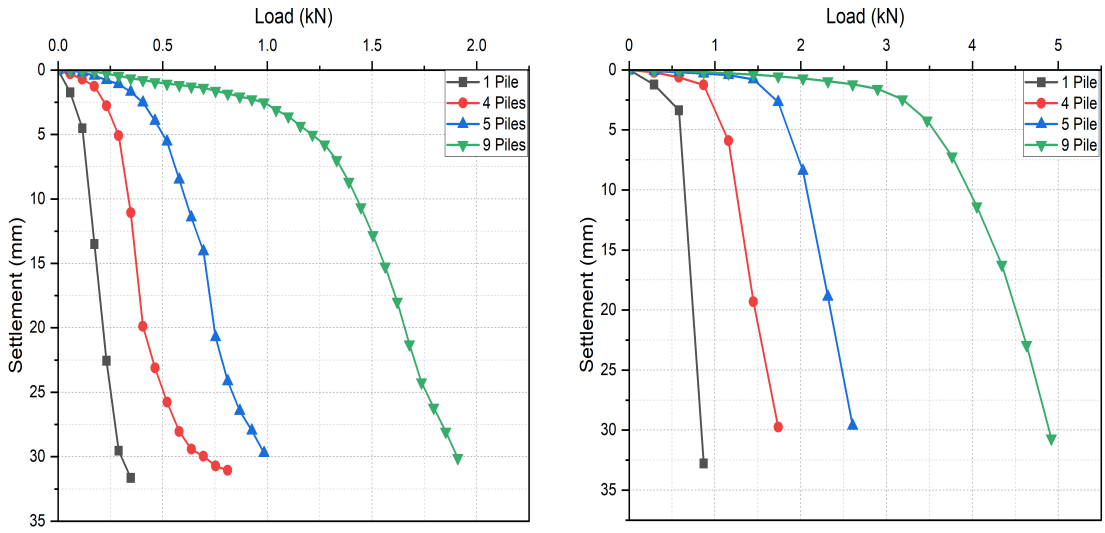

(a) Sand ($L_p = 360mm$) (b) Clay ($L_p = 360mm$)

Figure 4.14: Effect of number of piles in pile group

the pile group comprising of 9 piles carried more than 7 and 6 times higher load than a single pile. Similar to the piled-raft case, it was also found that the load-bearing capacity of the pile group improved with an increase in the number of piles. Moreover, the deviation in the curve after $30mm$ settlement indicates that the raft has made contact with the soil surface and has started taking loads.

4.4.4 Comparison between raft, piles and piled-raft

To study the combined behaviour of the raft and piles within a piled raft system, load-settlement curves depicting raft and group piles are plotted individually and then compared with the performance of piled raft. In the scenario involving group piles, attention was given to ensure that the piles remained freestanding, and that the bottom surface of the raft remained unsupported by the supporting soil. Conversely, when the raft was unpiled, it rested directly on the underlying soil, devoid of any pile attachment.

It was observed from Figures 4.15 and 4.16 that the combined load-bearing capacity of the raft and group piles does not match that of the piled-raft. This observation is further corroborated by findings in the literature (Elwakil and Azzam, 2016), which indicate that the load carried by the piled-raft either exceeds or equals the combined

load carried by the raft and the piles. This indeed results from the interactions between the foundation components and the supporting soil.

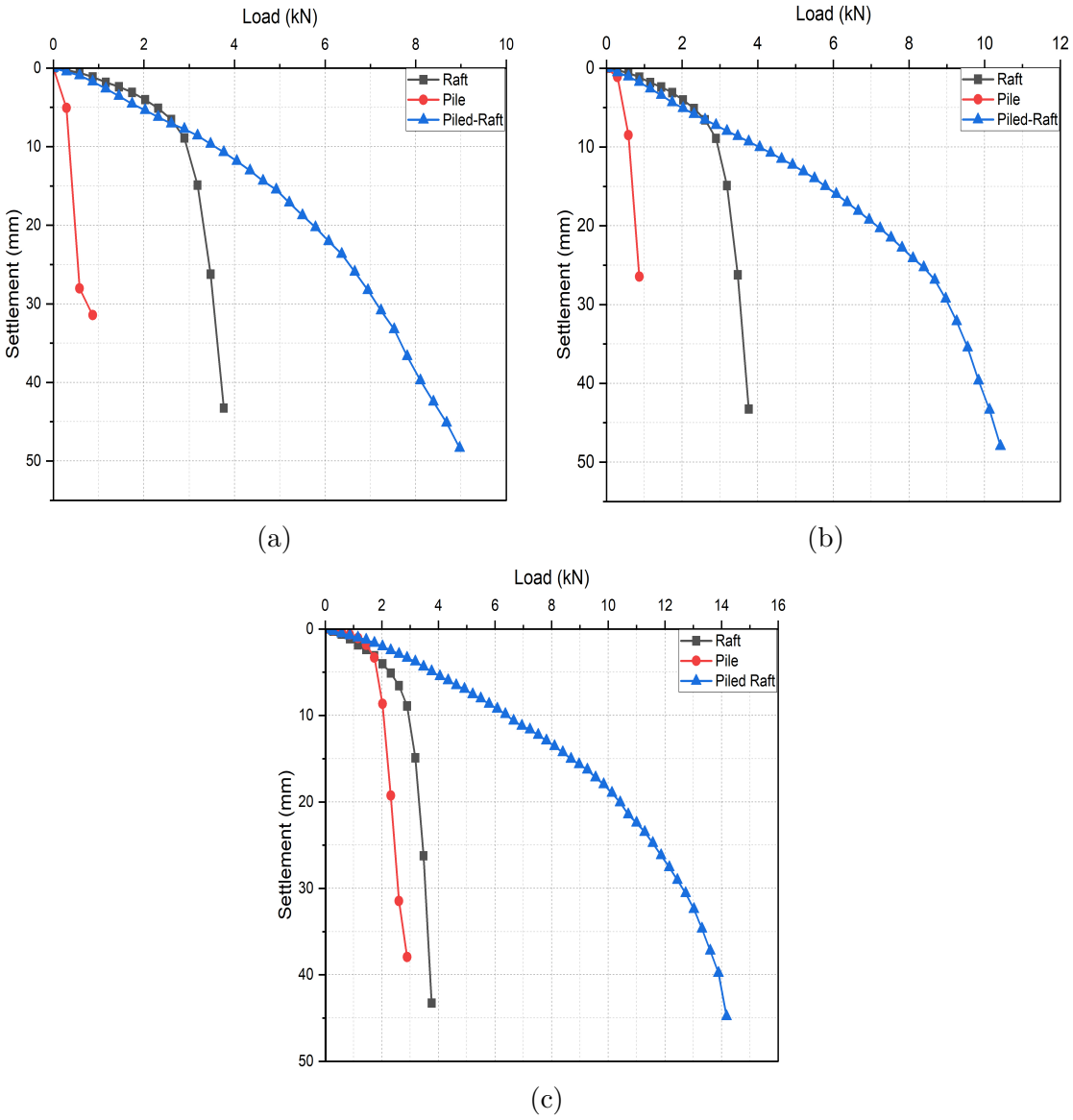

Figure 4.15: Comparison between raft, pile group and piled-raft in sand

Mathematically, the load-bearing capacity of the piled-raft system can be given by

$$Q_{PR} = Q_R + Q_P = \alpha_{pr} Q_{UR} + \alpha_{rp} Q_{PG} \tag{4.3}$$

Here, Q_R and Q_P represent the load that the raft and the piles are carrying. α_{pr} and α_{rp} are the interaction factors that characterize interactions between pile and raft and vice-versa, respectively. The subscripts UR, PG, and PR are unpiled-raft,

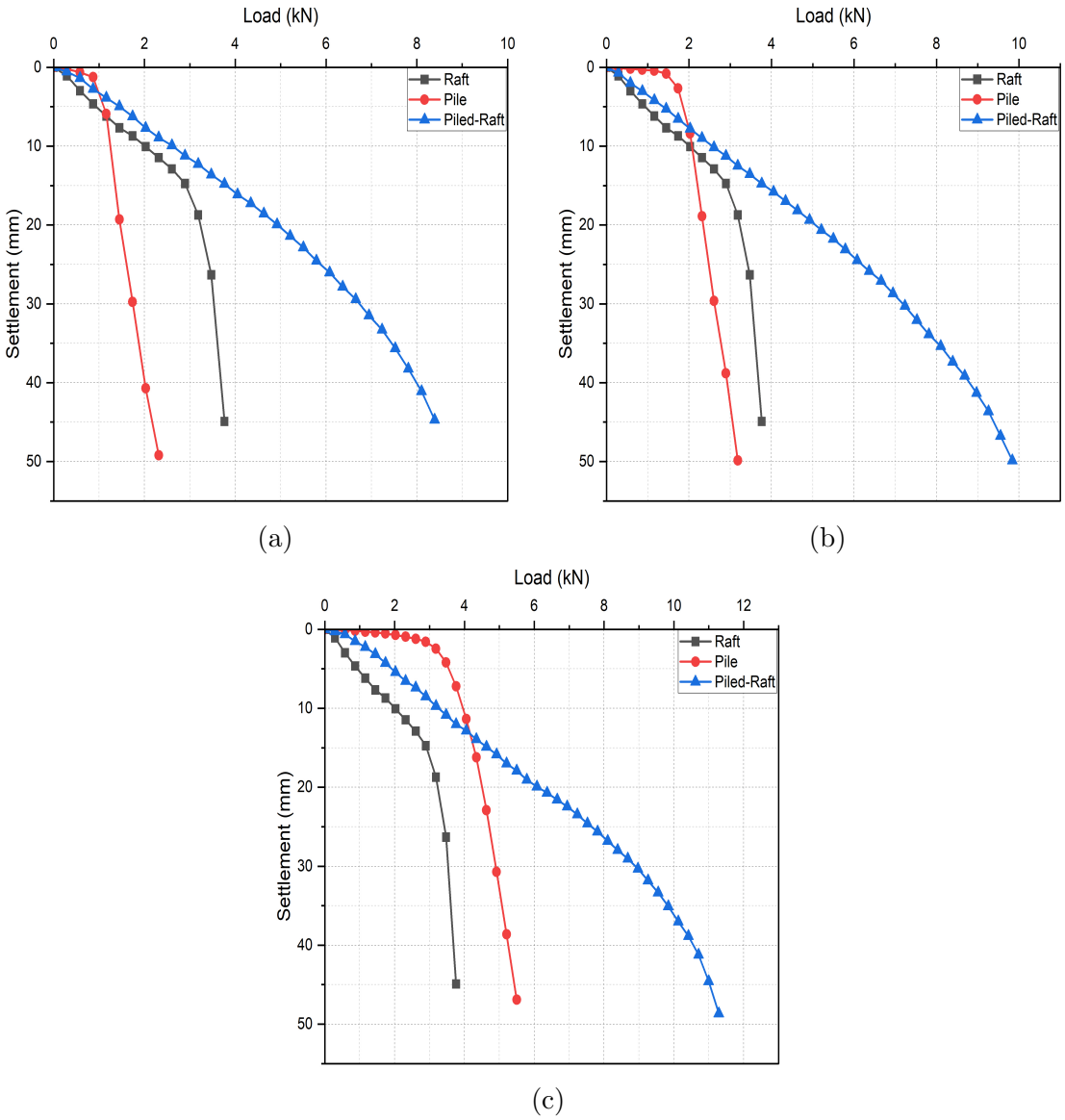

Figure 4.16: Comparison between raft, pile group and piled-raft in clay

pile group, and piled-raft, respectively, whereas Q represents the load capacity. The current chapter is dedicated exclusively to the experimental study, with a primary focus on investigating load sharing in piled rafts over sand and clay. It lays the foundation for a more comprehensive exploration in the subsequent chapter, which broadens the study's horizons by delving into the evaluation of interaction factors.

4.4.5 Load Improvement Ratio

An increase in the load-bearing capacity of the foundation due to the addition of piles can be defined by a dimensionless parameter known as load improvement ratio

(LIR). It is expressed as the ratio of the load carried by piled-raft (Q_{PR}) to that by the unpiled-raft (Q_{UR}) at constant settlement.

$$LIR = \frac{Q_{PR}}{Q_{UR}} \tag{4.4}$$

Figure 4.17 shows the variation of LIR with the relative settlement (s/B_r) in the case of sandy and clayey soil. Here, s denotes the raft settlement while B_r represents the raft width. It is observed that with an increase in the number of piles, LIR increases. Also, the LIR value is high at the early stages and decreases with an increase in settlement value. In the case of sand, the piled rafts with higher pile numbers show a sudden decrease initially and finally, after a certain value, such decrease becomes gradual. This implies the mobilization of piles after initial loading, leading to a reduction in LIR. Similar outcomes can be observed in earlier pieces of literature (Sosahab et al., 2019; Lee et al., 2015). Moreover, in the case of clay, the LIR values converge to roughly the same value regardless of the number of piles and do not significantly vary in later phases.

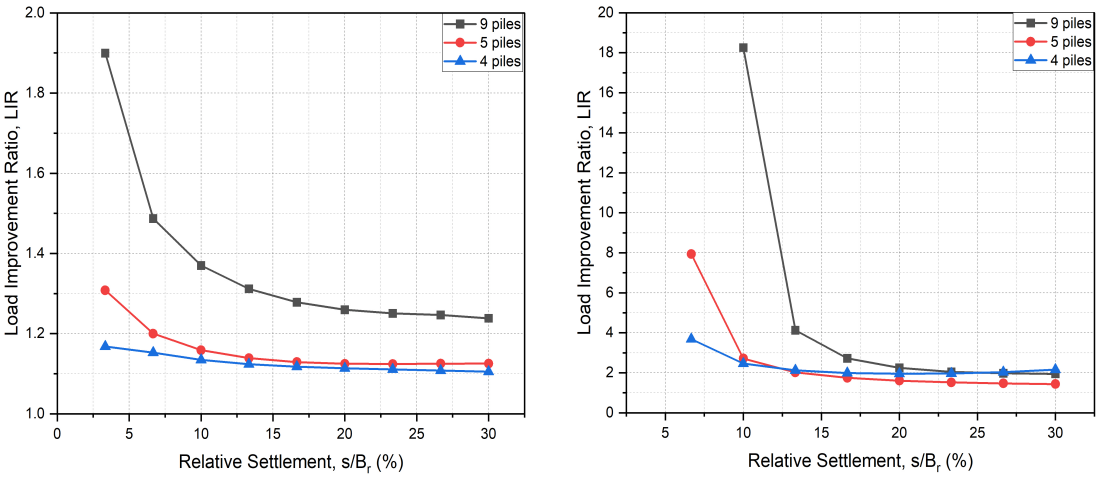

(a) Sand (b) Clay

Figure 4.17: Load Improvement Ratio

4.4.6 Load Sharing Ratio (α_p)

It is now widely accepted that the anticipated load from the superstructure is shared among the piles and the raft in pile-raft foundations. Such a complex load-sharing mechanism is governed mostly by the load-sharing ratio. The sharing ratio represents the load-sharing behaviour in piled-rafts and is usually defined as the percentage of the total load imposed on piled-raft (Q_{pr}) that is carried by piles (Q_p). It can be by the following expression:

$$\alpha_p = \frac{Q_p}{Q_{pr}} = 1 - \frac{Q_r}{Q_{pr}} \tag{4.5}$$

where Q_r and Q_p denote the load resisted by raft and piles, respectively. The variation of load sharing ratio for the present case of sand and clay with the settlement is depicted in Figures 4.18 and 4.19, respectively. Individual share of load carried by piles and the raft is presented for different configurations. The load share of a raft on sand is initially high and rises until it reaches a fixed limit. Even when there are a higher number of piles, the piles share of load is comparatively better but still less than the rafts share. Thus, it can be inferred that neglecting the load shared by rafts in the analysis process will not be wise.

It is evident that in the case of clay, the load share of piles is initially high, and gradually, the load is transferred to the raft at higher settlements. At initial settlement, the bottom of the raft had inadequate contact with the supporting clayey soil; hence, a lesser raft share is observed. On the contrary, since the piles are in direct contact with the soil, it leads to soil confinement and results in a higher proportion of pile share during initial settlement. The soil density beneath the raft increases as the piled-raft model settles more. Consequently, the raft and soil make better contact with each other, increasing the raft's share of the load. A higher percentage of load-sharing ratio can also be observed initially in the case of the piled raft with a greater number of piles due to the greater resistance offered by

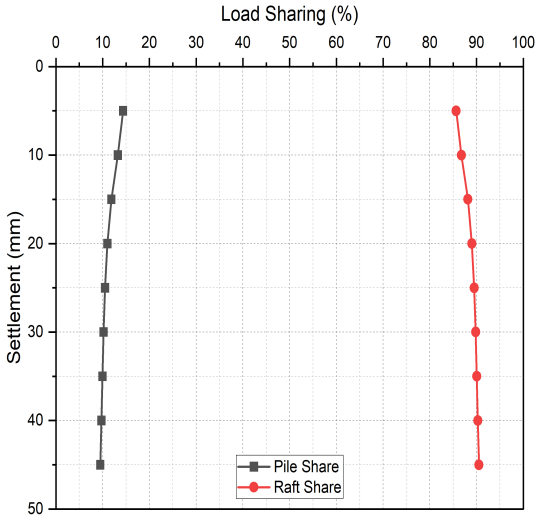

(a) No. of piles (n_p) = 4

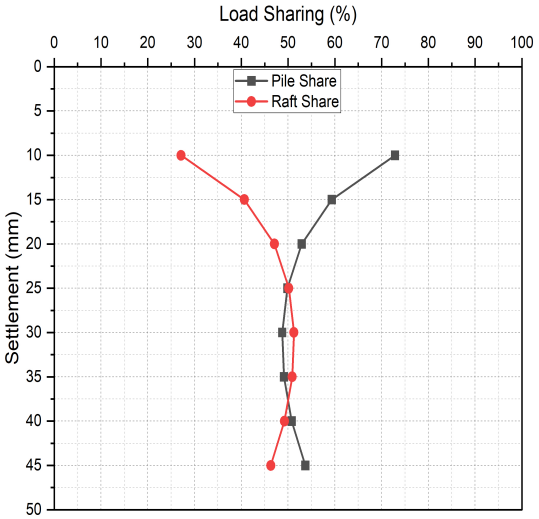

(a) No. of piles (n_p) = 4

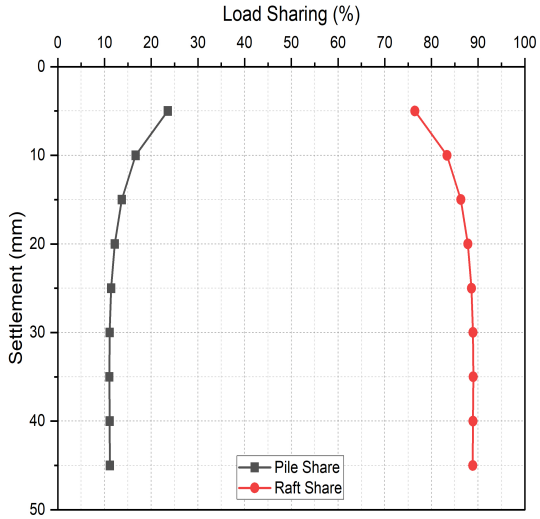

(b) No. of piles (n_p) = 5

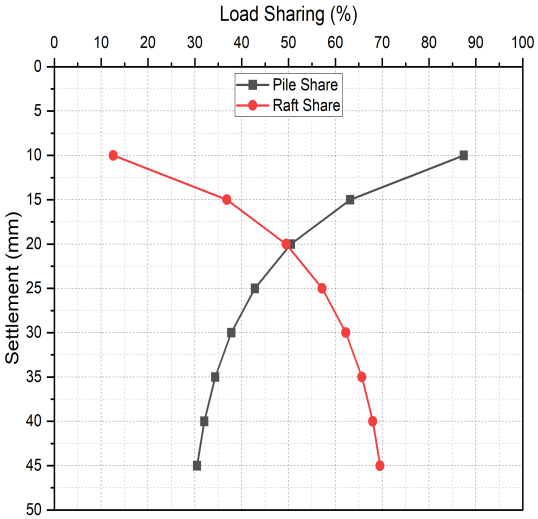

(b) No. of piles (n_p) = 5

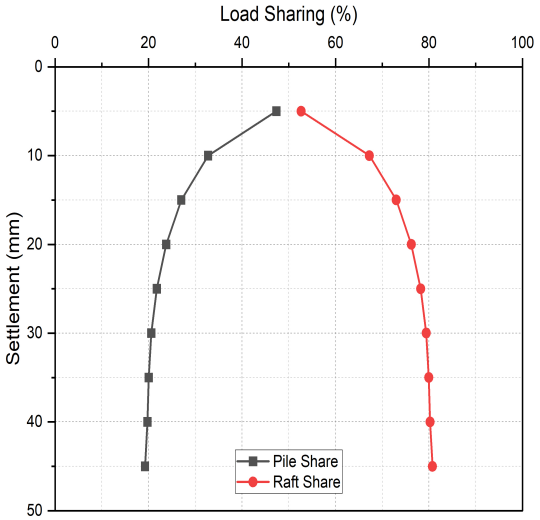

(c) No. of piles (n_p) = 9

Figure 4.18: Variation of load sharing in sand

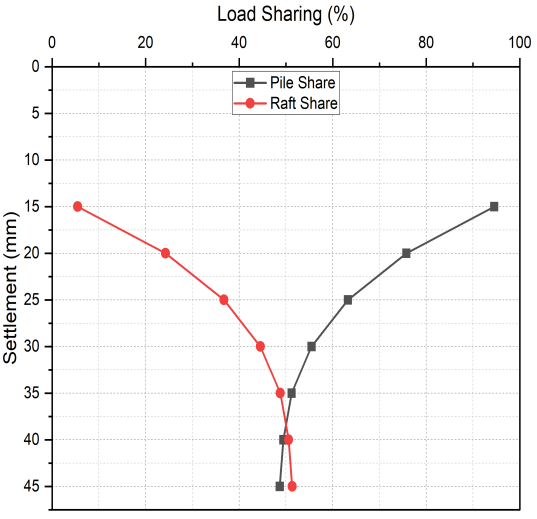

(c) No. of piles (n_p) = 9

Figure 4.19: Variation of load sharing in clay

them.

4.4.7 Comparison between experimental and numerical results

Figure 4.20 illustrates a comparison between experimental findings and numerical results obtained from Finite Element (FE) analysis. In this analysis, a piled raft model featuring 260mm long piles was employed. To validate the experimental data, two configurations were considered: one with a single pile and another with four piles.

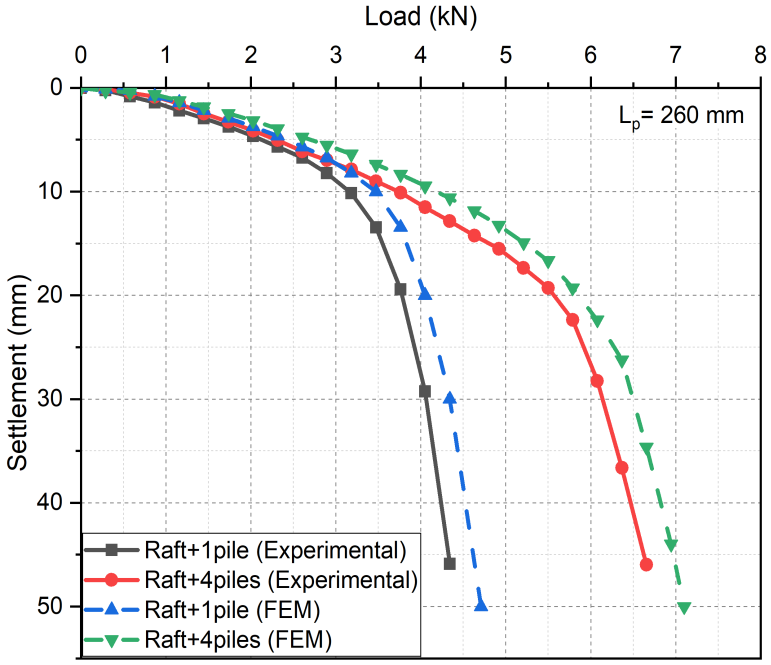

Figure 4.20: Comparison between experimental and numerical results

The figure reveals that the variations between the results fall within the range of 6% to 8%, generally remaining below 10%. This close correspondence between experimental and numerical outcomes strongly supports their reliability. Consequently, we can confidently rely on both sets of data to make informed predictions regarding the behaviour of piled rafts. The stress contour of the model with single pile is shown in figure 4.21.

Variations between experimental and numerical results in piled raft behaviour

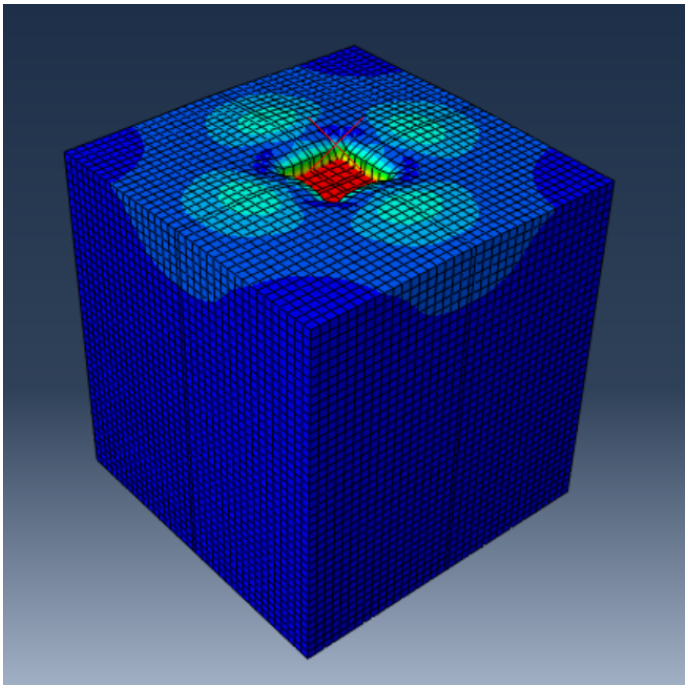

Figure 4.21: Stress contours of piled raft model with single pile ($L_p = 260mm$)

can arise from multiple factors, including simplifications in numerical models, discrepancies in material properties, variations in boundary conditions, geometric modelling, soil behaviour assumptions, load applications, experimental errors, numerical approximations, and real-world construction effects.

4.4.8 Limitations of the experimental study

The limitations of the experimental study encompass several factors:

- Dimensional Scaling: Scaling down model pile and raft dimensions from real-world counterparts can introduce inaccuracies due to the behavior of physical phenomena at smaller scales, potentially affecting findings' applicability to full-scale scenarios.

- Scaling Law Constraints: The study adheres to scaling laws, necessitating the use of scaled-down models. While valuable, these models may not fully replicate real-world behavior at full scale, possibly leading to scale-dependent discrepancies.

- In-situ Stress Representation: Replicating in-situ stress conditions accurately

in the testing tank is challenging. Differences between the laboratory setup and actual field conditions can impact the realism and relevance of experimental data.

- Soil Density Variability: Soil density variations across test scenarios may introduce uncertainties, affecting result comparability.

- Material Differences: The use of steel piles in experiments may not perfectly mimic the behavior of commonly used reinforced concrete (RC) piles. Material property differences can impact the accuracy of findings related to RC pile foundations.

- Soil Bin Deformation: Despite using a rigid soil bin, there's a risk of soil bin bulging or deformation under applied loads, potentially introducing unintended variations in test conditions and affecting result precision.

- Lab vs. Real-World: Experiments are conducted in a controlled laboratory setting, offering controlled conditions but differing from dynamic real-world scenarios. Findings may not fully reflect the complexities of real-world situations.

- Deviation from Natural Soil Conditions: The study employs artificial soil substitutes that may not perfectly replicate the intricate properties of natural soils. These substitutes could affect soil behaviour and may not capture all soil-specific nuances.

- Exclusion of Pore Pressure Effects: Pore pressure effects, which significantly influence soil behavior, are omitted from the experiments. This simplification may limit the study's ability to account for the full range of factors influencing piled-raft behaviour in practical applications.

Acknowledging these limitations is essential for interpreting the study's results accurately and for considering the applicability of its findings to real-world engineering scenarios

4.5 Summary

The present experimental research involves the analysis of piled-raft foundation systems through small-scale model tests. Parametric studies included the variation in the number and length of the piles. Given the relatively limited knowledge regarding the behavior of piled rafts on clayey soils, the study concurrently focuses on investigating their performance over both sand and clay. The research places particular emphasis on the examination of load improvement and load-sharing behavior in these scenarios.

Drawing upon the findings of the present experimental investigations and considering the associated limitations, the following conclusions can be derived:

- The validation of experimental results through numerical analysis in the present study (Figure 3.9) clearly demonstrates the potency of numerical analysis as a valuable tool for comparing and assessing outcomes.
- The observations from the current laboratory experiments demonstrate that piled rafts significantly mitigate settlement and offer greater resistance compared to raft foundations alone. This can be attributed to the fact that the piles bear the majority of the load within piled rafts.
- Even the addition of just a few piles to the raft significantly enhances the load-bearing capacity of the foundation, and this enhancement becomes more pronounced with an increase in the number of piles. In both the sand and clay cases, the observed raft capacity against a $40mm$ reference settlement remained consistently around $3.6kN$. However, in the sand scenario, improvements of up to $4.5kN, 8kN, 10kN$, and $14kN$ were observed for 1, 4, 5, and 9 piles, respectively. In the clay case, the load capacity increased from $3.6kN$ to $5.2kN, 7.9kN, 8.8kN$, and $10.2kN$ for the same respective pile numbers.
- Piled rafts featuring longer piles tend to demonstrate higher bearing capacities.

In the current scenario, the load-bearing capacities for the longest pile length showed an impressive increase of up to 300%. To put this into perspective, when compared to an unpiled raft carrying a load of $3.6kN$, a piled-raft with 9 piles and a $360mm$ pile length exhibited remarkable resistance, with values of approximately $13.8kN$ and $10.6kN$ in the sand and clay cases, respectively.

- The load improvement ratio (LIR) increases with an increasing number of piles. Notably, LIR tends to be more pronounced in the early stages of loading and diminishes as the settlement value increases, indicating mobilization of piles after the initial loading.

- The findings also demonstrated that the raft significantly contributed to the load sharing in piled-raft foundations. Therefore, it is vital to acknowledge the raft's importance in the analysis and design of such foundations.

- In the majority of cases, piled rafts over clay exhibited patterns resembling those over sand. However, it was found that the raft contributed a larger portion of the load in the sand than in clay. Raft's share of the load in sand reached about 90% when piles were lesser and decreased as the pile numbers increased. In the clay case, the influence of the piles on load sharing was higher, and the raft's share improved with the settlement.

- The experimental findings also revealed that the load-bearing capacity of the combined piled-raft system is greater than the simple addition of the load capacities of the raft and the piles, hence proving its complex behaviour of load-sharing. Such complexity arises due to the interactions between soil and the foundation components. Moreover, these interactions considerably impact the behaviour of piled rafts.

- To restrict the maximum settlement, an optimization of the piled-raft geometries should be established to prevent an irrational and uneconomical design.

- The current study is confined to testing piled-raft behavior under normal

gravitational conditions (1g), limiting its ability to fully capture real-world behaviors. Nonetheless, centrifuge tests present a compelling alternative. These tests apply increased gravitational forces to models, replicating conditions impossible to achieve under standard gravity. Centrifuge testing enables a more comprehensive and realistic analysis of piled-raft behavior, facilitating deeper insights into its performance across different conditions, often unattainable through conventional 1g testing.